Supplemental Material for "Sources of Seasonal Sea Ice Bias for CMIP6 Models in the Hudson Bay Complex"

Alex D. Crawford, Erica Rosenblum, Jennifer V. Lukovich, Julienne C. Stroeve

Corresponding author: Alex D. Crawford, alex.crawford@umanitoba.ca

Table S1: CMIP6 Models used in this study. X's mark models for which at least one of required variable(s) for each property was unavailable at the necessary temporal resolution from historical simulations when data were acquired in summer 2022. (All listed models provide daily sea ice concentration output.) The three models used to estimate internal variability (23 replicates each) are in bold.

Model	Citation	Sea Ice Thickness & Dynamics	Surface Air & Ocean Temp.	Surface Wind	Albedo	Snow Depth
ACCESS-CM2	Bi et al. (2020)					
AWI-CM-1-1-MR	Semmler et al. (2020)				X	
AWI-ESM-1-1-LR	Semmler et al. (2020)					
BCC-CSM2-MR	Wu et al. (2021)					
BCC-ESM1	Wu et al. (2020)					
CanESM5	Swart et al. (2019)	X				
CESM2	Danabasoglu et al. (2020)			X		
CESM2-FV2	Danabasoglu et al. (2020)			X		
CESM2-WACCM	Danabasoglu et al. (2020)			X		
CESM2-WACCM-FV2	Danabasoglu et al. (2020)			X		
CMCC-CM2-HR4	Cherchi et al. (2019)	X				X
CMCC-CM2-SR5	Cherchi et al. (2019)				X	
CMCC-ESM2	Lovato et al. (2022)					
CNRM-CM6-1	Saint-Martin et al. (2021)					
CNRM-CM6-1-HR	Saint-Martin et al. (2021)					
CNRM-ESM2-1	Séférian et al. (2019)					
EC-Earth3	Döscher et al. (2021)					
EC-Earth3-AerChem	Döscher et al. (2021)					

Model	Citation	Sea Ice Thickness & Dynamics	Surface Air & Ocean Temp.	Surface Wind	Albedo	Snow Depth
EC-Earth3-CC	Döscher et al. (2021)					
EC-Earth3-Veg	Döscher et al. (2021)					
EC-Earth3-Veg-LR	Döscher et al. (2021)					
GFDL-CM4	Held et al. (2019)	X			X	
ICON-ESM-LR	Jungclaus et al. (2022)					
IPSL-CM5A2-INCA	Sepulchre et al. (2020)					X
IPSL-CM6A-LR	Boucher et al. (2020)					
IPSL-CM6A-LR-INCA	Boucher et al. (2020)	X				
KIOST-ESM	Pak et al. (2021)	X				X
MIROC-ES2L	Hajima et al. (2020)					
MIROC6	Tatebe et al. (2019)					
MPI-ESM1-2-HR	Müller et al. (2018)					
MPI-ESM1-2-LR	Mauritsen et al. (2019)					
MRI-ESM2-0	Yukimoto et al. (2019)					
NESM3	Cao et al. (2018)					
NorESM2-LM	Seland et al. (2020)			X		
NorESM2-MM	Seland et al. (2020)			X		
SAM0-UNICON	Park et al. (2019)	X		X		
UKESM1-0-LL	Sellar et al. (2019)	X				

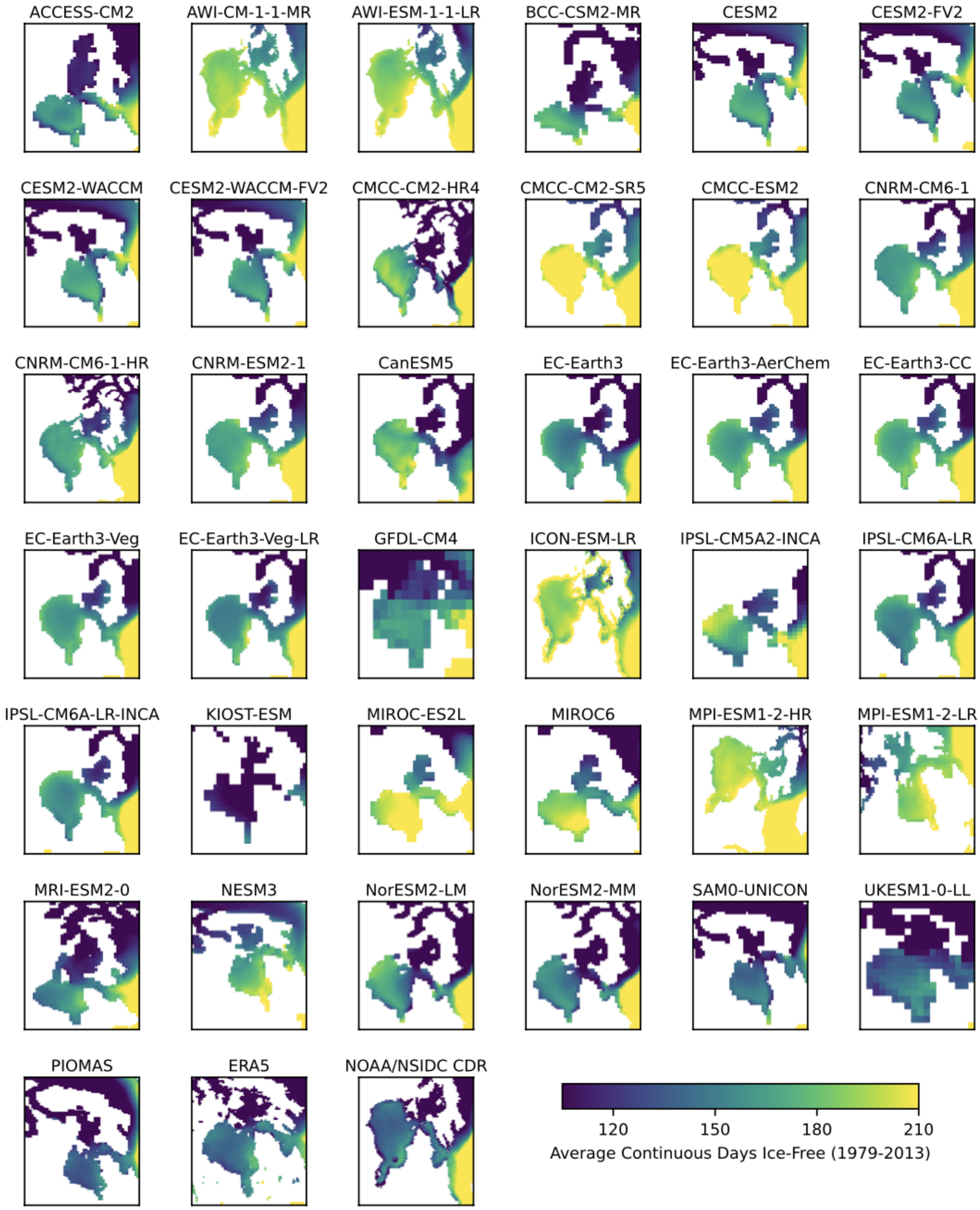

Fig. S1: Average continuous ice-free period on native model grids (1979-2014) in the HBC, using the first replicate of each CMIP6 model. Also shown are the averages from the PIOMAS and ERA5 reanalyses and the NOAA/NSIDC CDR (based on passive microwave observations).

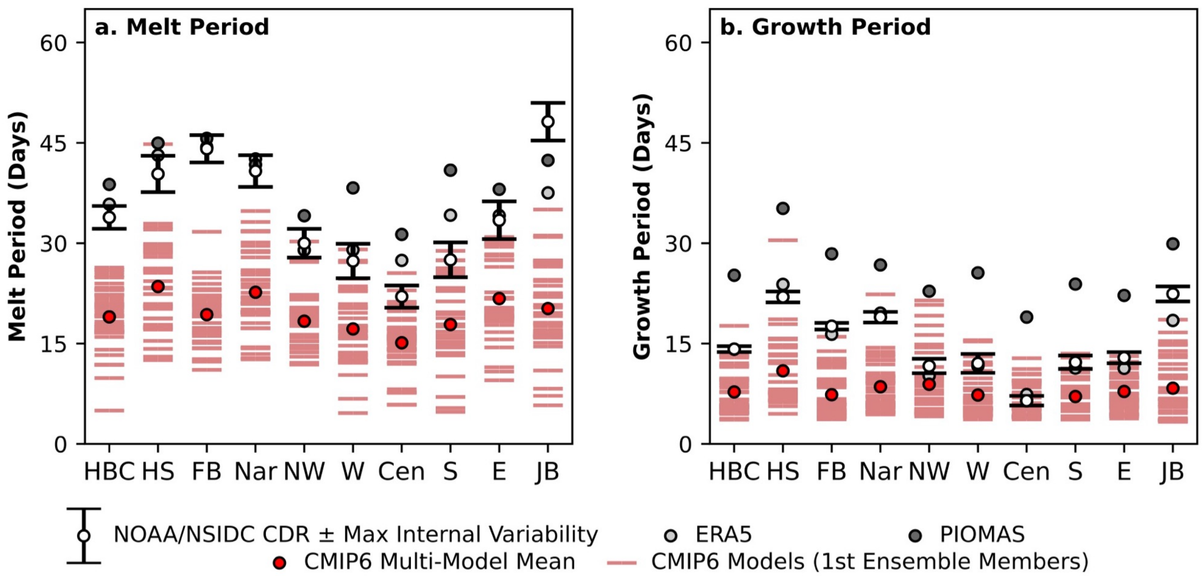

Fig. S2: **Melt period and growth period of sea ice in HBC (1979-2014).** As in Figure 2, but for the melt period (days between opening (SIC < 80%) and retreat (SIC < 15%)) and the growth period (days between advance (SIC ≥ 15%) and closing (SIC ≥ 80%)).

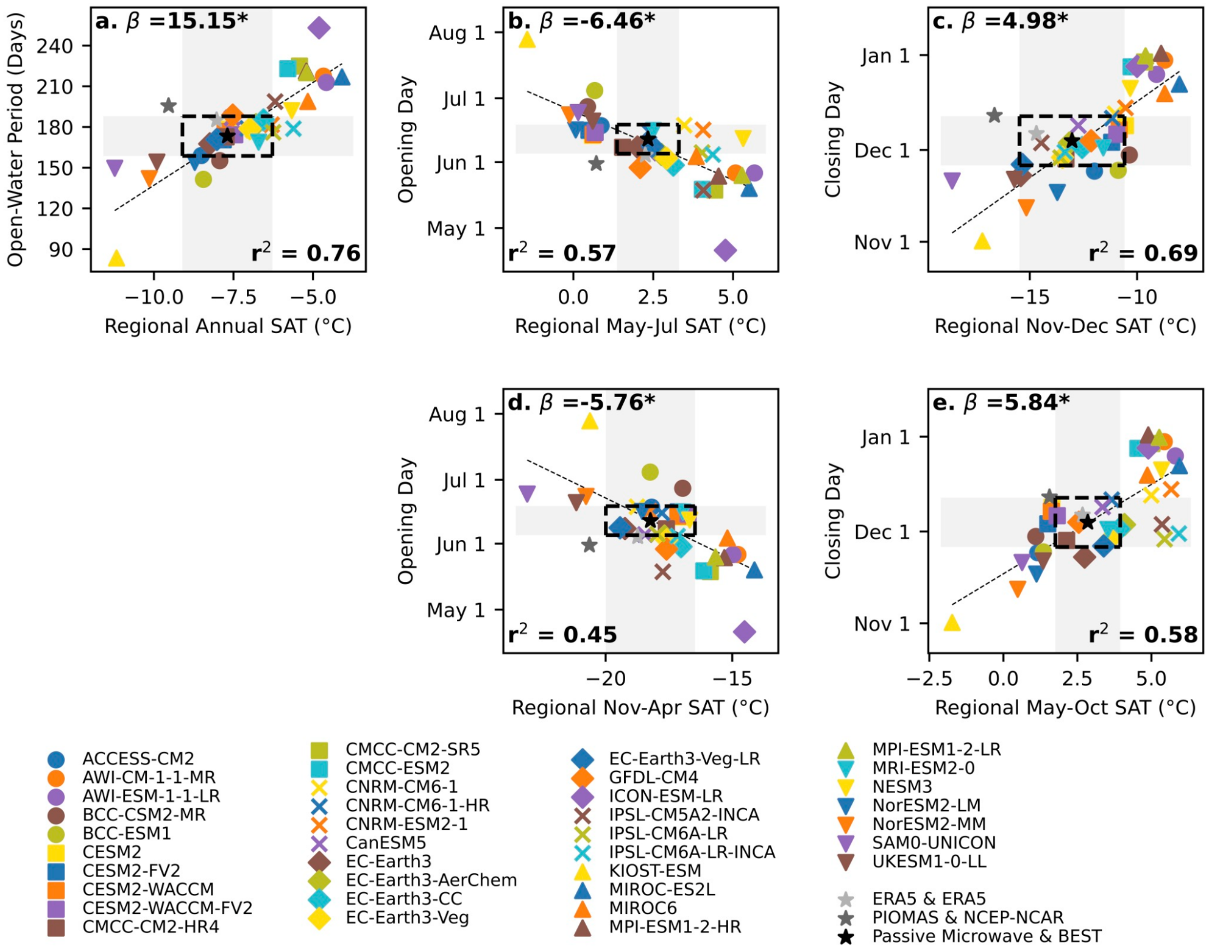

Fig. S3: Scatter plots of HBC sea ice phenology versus average temperature (1979-2014). Temperature is averaged annually for the open-water period (a,d), during the melt period (b) or the prior ice-covered period (e) for the opening day, and during the growth period (c) or prior ice-free period (f) for the closing day. All temperature aggregation is for the HBC region except (d), for which averaging is global.

Black dashed boxes represent the range of internal variability ($\mu_{obs} \pm 2\sigma_{max}$). The dotted gray line represents the ordinary least-squares regression of each phenology variable against temperature. The slope of that line is printed at the top of each graph, and an asterisk indicates a significant trend ($p < 0.05$).

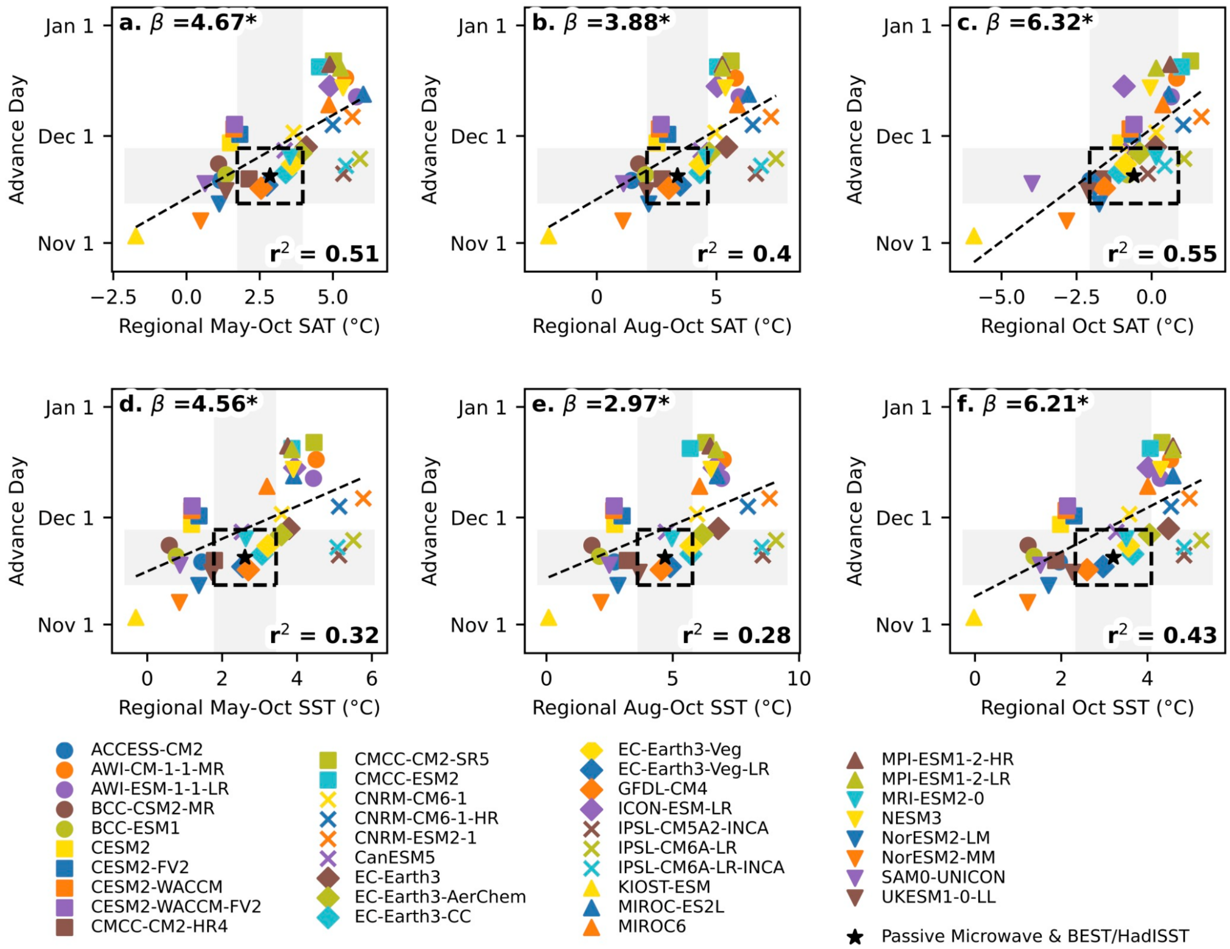

Fig. S4: Scatter plots of HBC sea ice advance day versus average temperature (1979-2014). Surface temperature of the atmosphere (a-c) and ocean (d-f) is averaged for the ice melt and ice-free period (a,d), just the ice-free period (b,e) or October (c,f). All temperature aggregation is for HBC region. Solid black boxes represent the range of internal variability ($\mu_{obs} \pm 2\sigma_{max}$). The black dashed line represents the ordinary least-squares regression of sea ice advance day against temperature. The slope of that line is printed at the top of each graph, and an asterisk indicates a significant trend ($p < 0.05$).

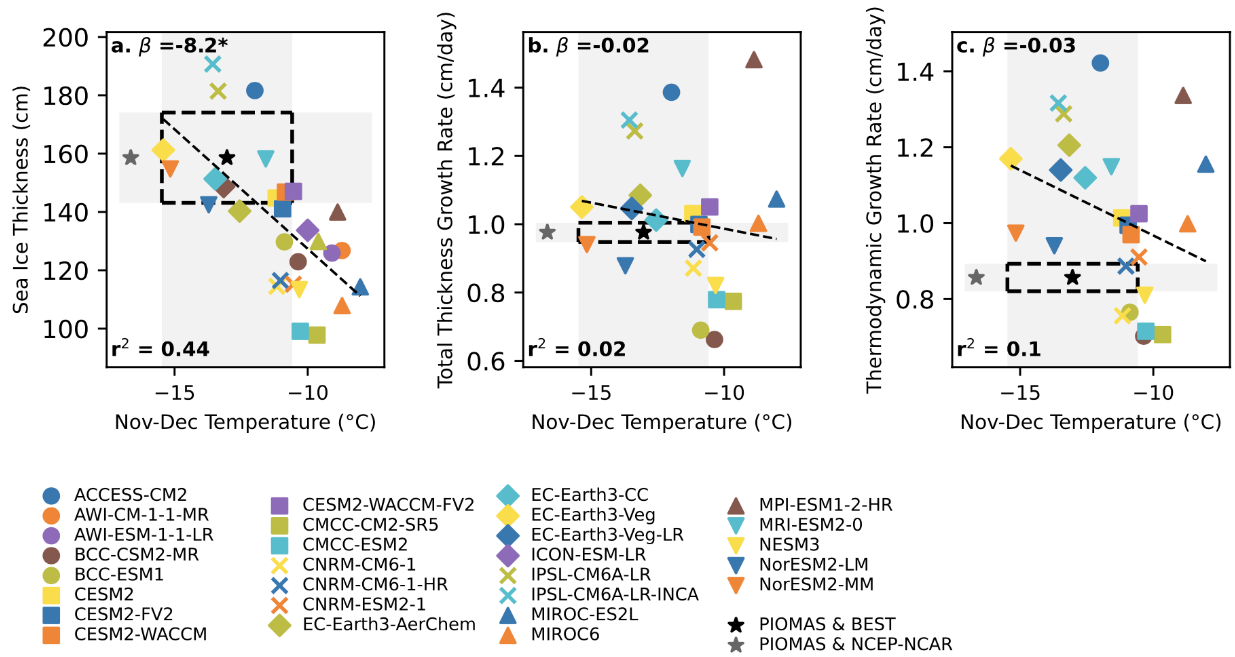

Fig. S5: Scatter plots of sea ice growth versus autumn temperature (1979-2014) for the entire HBC. Sea ice growth is defined by (a) the average April thickness, (b) the average rate of change in sea ice thickness from November to April, and (c) thermodynamic thickness change from November to April. Black dashed boxes and gray shading represent the range of internal variability ($\mu_{obs} \pm 2\sigma_{max}$). The dotted black line represents the ordinary least-squares regression of the y variables against temperature. The slope of that line is printed at the top of each graph, and an asterisk indicates a significant trend ($p < 0.05$).

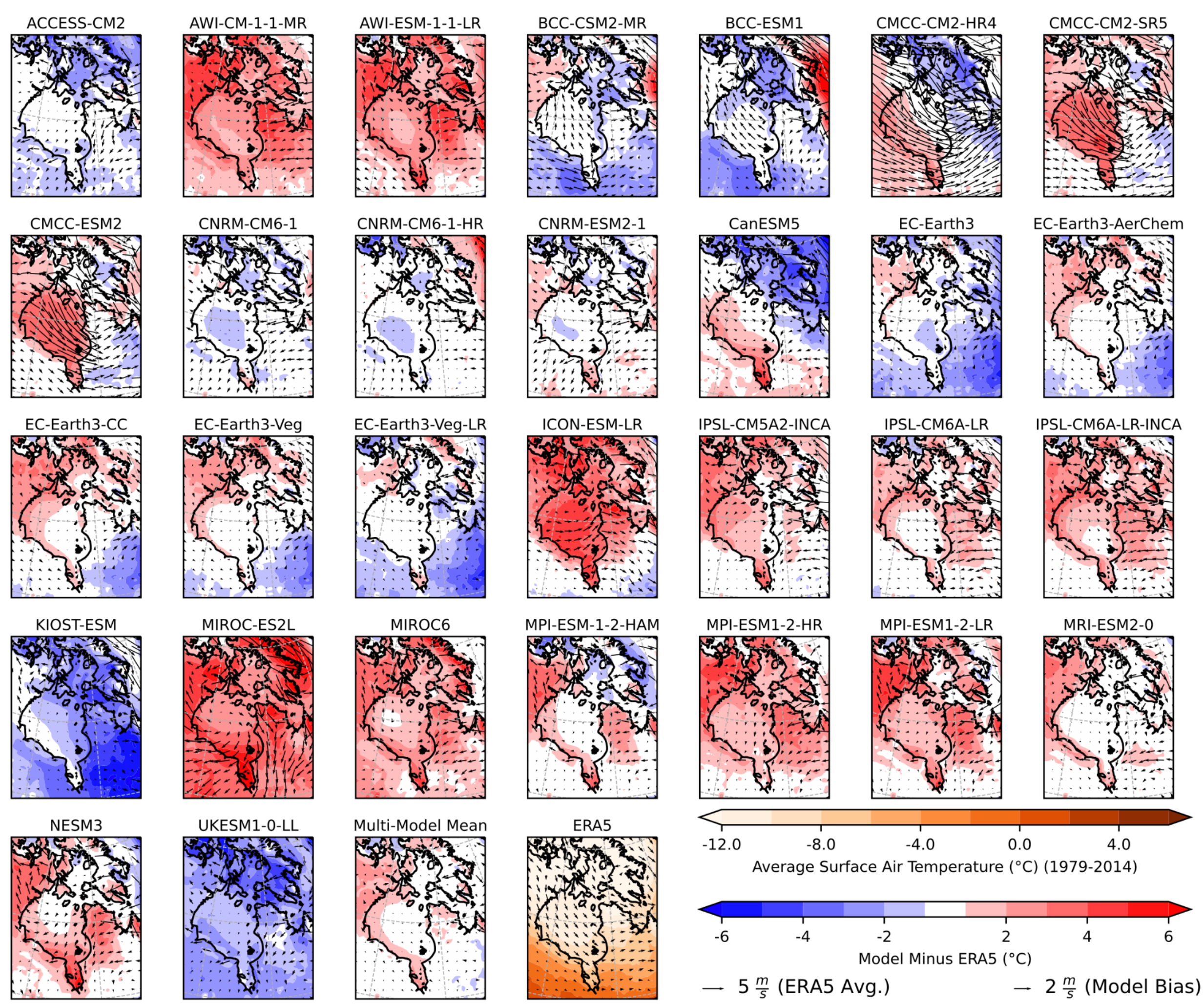

Fig. S6: Model bias in 2-m air temperature and 10-m wind vectors during January-July (1979-2014), which roughly corresponds to the ice-covered season and melt season in HBC.

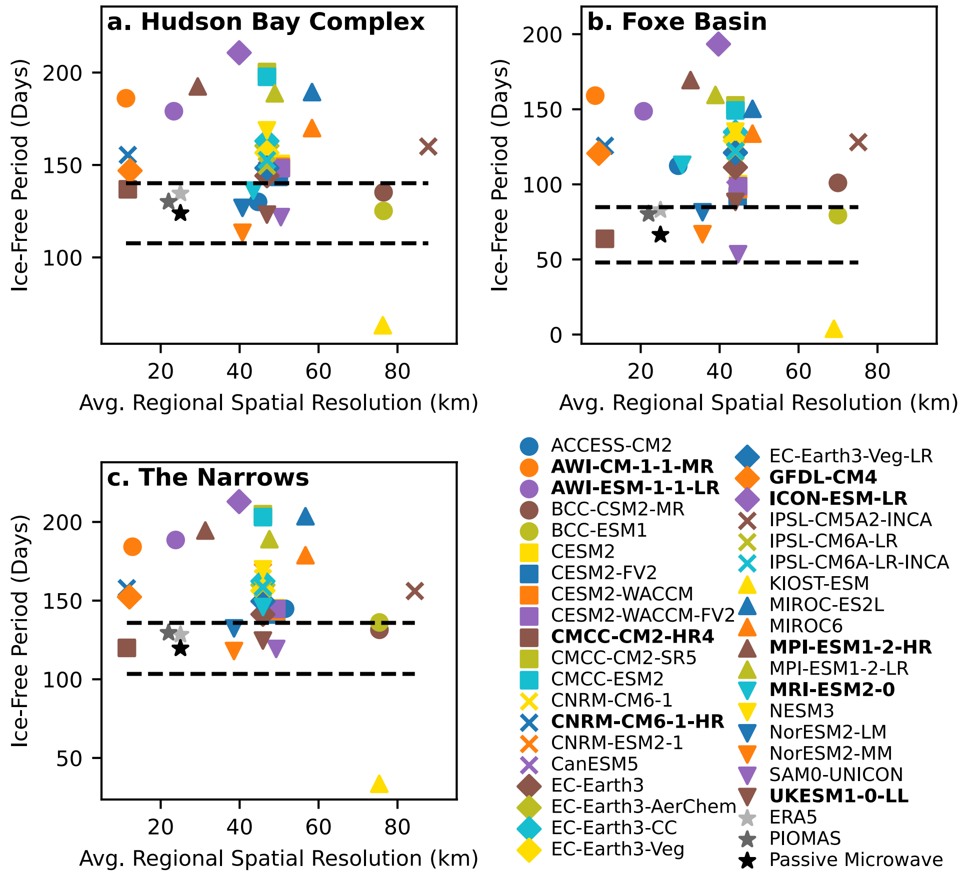

Fig. S7: Scatter plots of the average ice-free period (1979-2014) versus average regional spatial resolution of the ocean grid in (a) HBC, (b) Foxe Basin, and (c) the Narrows. Black dashed lines represent the range of internal variability ($\mu_{obs} \pm 2\sigma_{max}$). Models listed in bold in the legend are those which include Fury and Hecla Strait. Despite the vast range of spatial resolution in these models, finer-resolution models do not perform demonstrably better than their coarser counterparts.

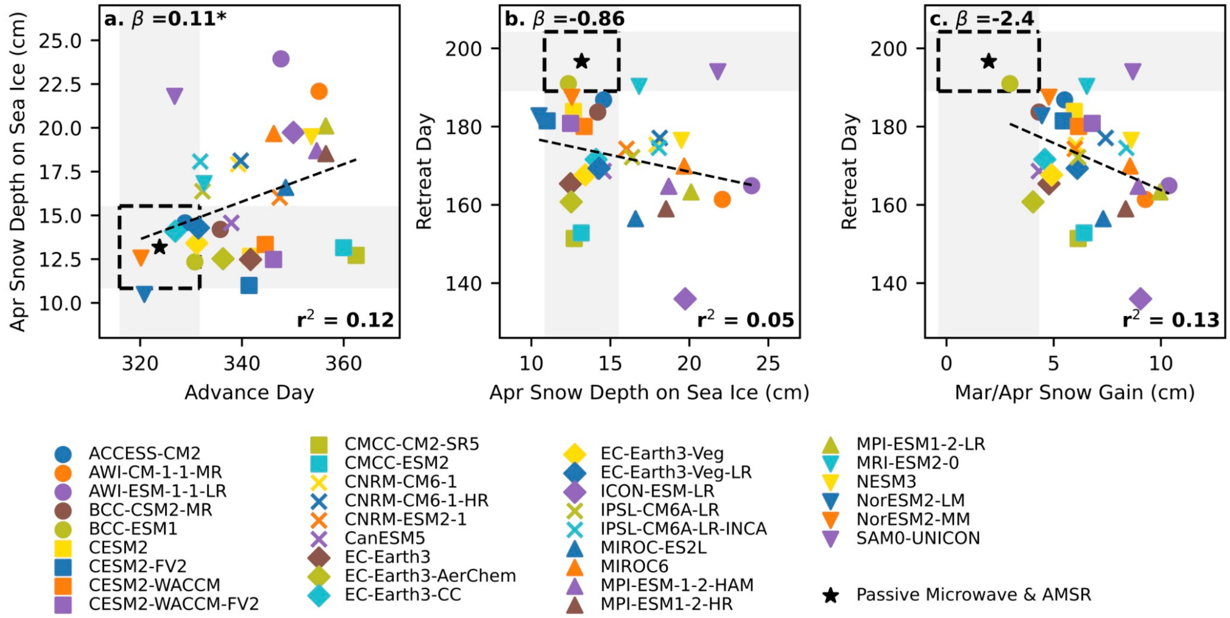

Fig. S8: Relationship between sea ice phenology and snow depth on sea ice in HBC (1979-2014). (a) Models with later advance day typically have *deeper* snow packs come April despite a shorter ice-covered period. (b) Several models have too much snow of sea ice in April (the last month of the ice-covered season), but this has no clear bearing on retreat day. (c) Snow depth increase during March and April (which is more likely to impact surface albedo) also has no clear relationship with retreat day, although most models have too much snow gain.

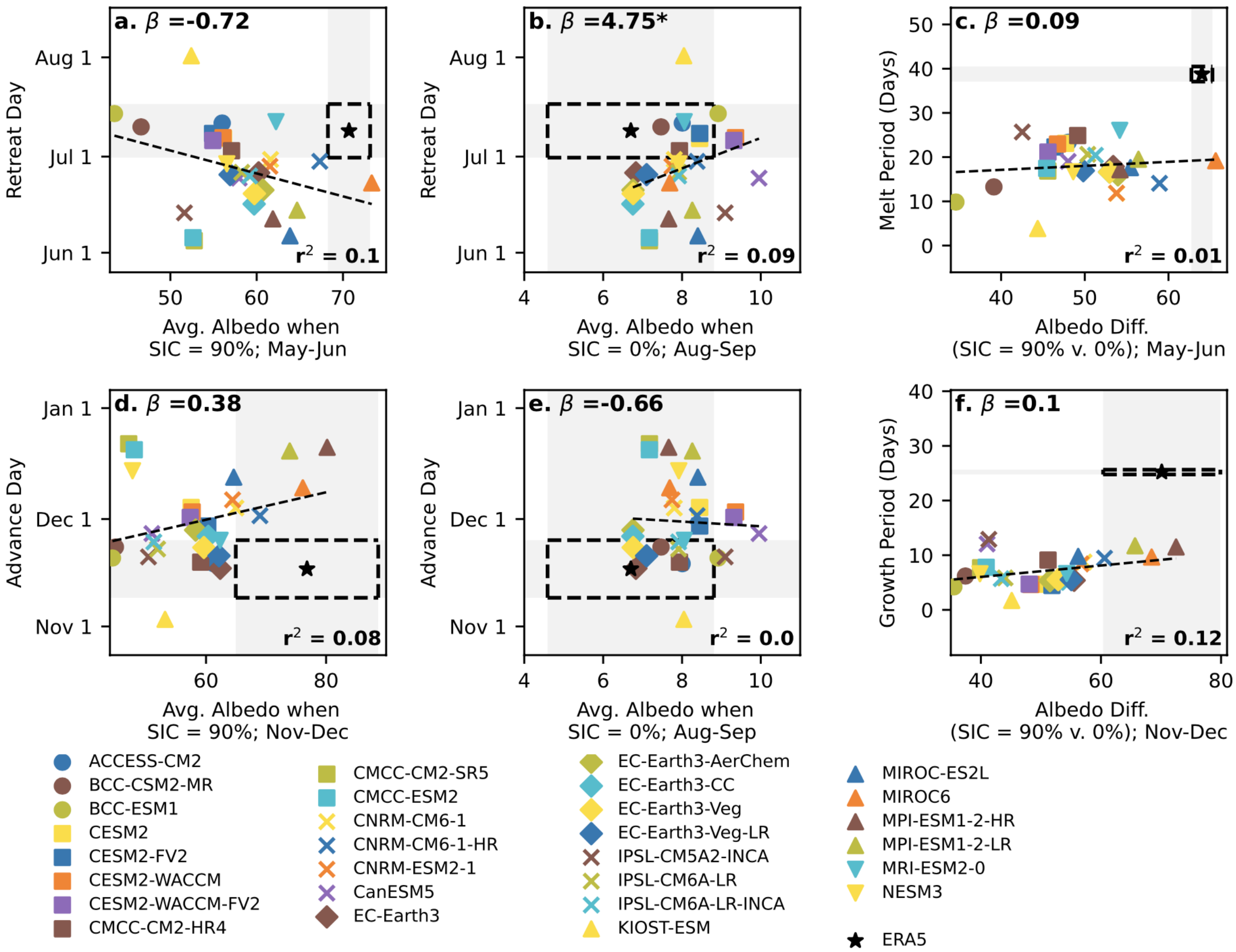

Fig. S9: Scatter plots of sea ice phenology versus surface albedo in HBC (1979-2014). Average retreat day in each model is compared to sea ice albedo during May-June (a), and advance day is compared to sea ice albedo during Nov-Dec (b). Both retreat and advance are also compared to the albedo of open water (c,e). The melt period (c) and growth period (f) are compared to the difference in albedo between sea ice and open water in the appropriate season. Note that SIC of 90% is used instead of 100% because few instances of SIC at 100% exist in either models or observations. Black dashed boxes and gray shading represent the range of internal variability ($\mu_{obs} \pm 2\sigma_{max}$). The dotted black line represents the ordinary least-squares regression of period length against sensitivity. (Neither coefficient is significant at $p < 0.05$.)

There also is no significant relationship between a model's growth period or melt period and the difference between albedo of the sea ice and ocean.

References

Bi D and 18 others (2020) Configuration and spin-up of ACCESS-CM2, the new generation Australian Community Climate and Earth System Simulator Coupled Model. *Journal of Southern Hemisphere Earth Systems Science* 70(1), 225. doi:10.1071/es19040.

Boucher O and 79 others (2020) Presentation and Evaluation of the IPSL-CM6A-LR Climate Model. *Journal of Advances in Modeling Earth Systems* 12(7). doi:10.1029/2019ms002010.

Cao J and 10 others (2018) The NUIST Earth System Model (NESM) version 3: description and preliminary evaluation. *Geoscientific Model Development* 11(7), 2975–2993. doi:10.5194/gmd-11-2975-2018.

Cherchi A and 10 others (2019) Global Mean Climate and Main Patterns of Variability in the CMCC-CM2 Coupled Model. *Journal of Advances in Modeling Earth Systems* 11(1), 185–209. doi:10.1029/2018ms001369.

Danabasoglu G and 42 others (2020) The Community Earth System Model Version 2 (CESM2). *Journal of Advances in Modeling Earth Systems* 12(2). doi:10.1029/2019ms001916.

Döscher R and 61 others (2021) The EC-Earth3 Earth System Model for the Climate Model Intercomparison Project 6. *Geoscientific Model Development Discussions* 2021, 1–90. doi:10.5194/gmd-2020-446.

Hajima T and 14 others (2020) Development of the MIROC-ES2L Earth system model and the evaluation of biogeochemical processes and feedbacks. *Geoscientific Model Development* 13(5), 2197–2244. doi:10.5194/gmd-13-2197-2020.

Held IM and 44 others (2019) Structure and Performance of GFDL's CM4.0 Climate Model. *Journal of Advances in Modeling Earth Systems* 11(11), 3691–3727. doi:10.1029/2019ms001829.

Jungclaus JH and 40 others (2022) The ICON Earth System Model Version 1.0. *Journal of Advances in Modeling Earth Systems* 14(4). doi:10.1029/2021ms002813.

Lovato T and 11 others (2022) CMIP6 Simulations With the CMCC Earth System Model (CMCC-ESM2). *Journal of Advances in Modeling Earth Systems* 14(3). doi:10.1029/2021ms002814.

Mauritsen T and 68 others (2019) Developments in the MPI-M Earth System Model version 1.2 (MPI-ESM1.2) and Its Response to Increasing CO2. *Journal of Advances in Modeling Earth Systems* 11(4), 998–1038. doi:10.1029/2018ms001400.

Müller WA and 20 others (2018) A Higher-resolution Version of the Max Planck Institute Earth System Model (MPI-ESM1.2-HR). *Journal of Advances in Modeling Earth Systems* 10(7), 1383–1413. doi:10.1029/2017ms001217.

Pak G and 14 others (2021) Korea Institute of Ocean Science and Technology Earth System Model and Its Simulation Characteristics. *Ocean Science Journal* 56(1), 18–45. doi:10.1007/s12601-021-00001-7.

Park S, Shin J, Kim S, Oh E and Kim Y (2019) Global Climate Simulated by the Seoul National University Atmosphere Model Version 0 with a Unified Convection Scheme (SAM0-UNICON) Global Climate Simulated by the Seoul National University Atmosphere Model

Version 0 with a Unified Convection Scheme (SAM0-UNICON). *Journal of Climate* 32(10), 2917–2949. doi:10.1175/jcli-d-18-0796.1.

Saint-Martin D and 16 others (2021) Tracking Changes in Climate Sensitivity in CNRM Climate Models. *Journal of Advances in Modeling Earth Systems* 13(6). doi:10.1029/2020ms002190.

Séférian R and 31 others (2019) Evaluation of CNRM Earth System Model, CNRM-ESM2-1: Role of Earth System Processes in Present-Day and Future Climate. *Journal of Advances in Modeling Earth Systems* 11(12), 4182–4227. doi:10.1029/2019ms001791.

Seland Ø and 29 others (2020) Overview of the Norwegian Earth System Model (NorESM2) and key climate response of CMIP6 DECK, historical, and scenario simulations. *Geoscientific Model Development* 13(12), 6165–6200. doi:10.5194/gmd-13-6165-2020.

Sellar AA and 50 others (2019) UKESM1: Description and Evaluation of the U.K. Earth System Model. *Journal of Advances in Modeling Earth Systems* 11(12), 4513–4558. doi:10.1029/2019ms001739.

Semmler T and 13 others (2020) Simulations for CMIP6 With the AWI Climate Model AWI-CM-1-1. *Journal of Advances in Modeling Earth Systems* 12(9). doi:10.1029/2019ms002009.

Sepulchre P and 27 others (2020) IPSL-CM5A2 – an Earth system model designed for multi-millennial climate simulations. *Geoscientific Model Development* 13(7), 3011–3053. doi:10.5194/gmd-13-3011-2020.

Swart NC and 21 others (2019) The Canadian Earth System Model version 5 (CanESM5.0.3). *Geoscientific Model Development* 12(11), 4823–4873. doi:10.5194/gmd-12-4823-2019.

Tatebe H and 24 others (2019) Description and basic evaluation of simulated mean state, internal variability, and climate sensitivity in MIROC6. *Geoscientific Model Development* 12(7), 2727–2765. doi:10.5194/gmd-12-2727-2019.

Wu T and 13 others (2020) Beijing Climate Center Earth System Model version 1 (BCC-ESM1): model description and evaluation of aerosol simulations. *Geoscientific Model Development* 13(3), 977–1005. doi:10.5194/gmd-13-977-2020.

Wu T and 29 others (2021) BCC-CSM2-HR: a high-resolution version of the Beijing Climate Center Climate System Model. *Geoscientific Model Development* 14(5), 2977–3006. doi:10.5194/gmd-14-2977-2021.

Yukimoto S and 16 others (2019) The Meteorological Research Institute Earth System Model Version 2.0, MRI-ESM2.0: Description and Basic Evaluation of the Physical Component. *Journal of the Meteorological Society of Japan. Ser. II* 97(5), 931–965. doi:10.2151/jmsj.2019-051.